Biochimica et Biophysica Acta 1798 (2010) 453–460

Contents lists available at ScienceDirect

Biochimica et Biophysica Acta

journal homepage: www.elsevier.com/locate/bbamem

Characterization of membrane properties of inositol phosphorylceramide

Anders Björkbom [a,*], Henna Ohvo-Rekilä [a], Pasi Kankaanpää [b], Thomas K.M. Nyholm [a], Bodil Westerlund [a], J. Peter Slotte [a]

[a] Department of Biochemistry and Pharmacy, Åbo Akademi University, Tykistökatu 6 A, FI-20520, Finland
[b] Department of Biochemistry and Food Chemistry, University of Turku, FI-20014 Turku, Finland

ARTICLE INFO

Article history:
Received 5 August 2009
Received in revised form 5 October 2009
Accepted 4 November 2009
Available online 11 November 2009

Keywords:
Sphingolipid
Ordered domain
Calcium effect
Vesicle aggregation
Cholesterol

ABSTRACT

Inositol phosphorylceramides (IPCs) are a class of anionic sphingolipids with a single inositol-phosphate head group coupled to ceramide. IPCs and more complex glycosylated IPCs have been identified in fungi, plants and protozoa but not in mammals. IPCs have also been identified in detergent resistant membranes in several organisms. Here we report on the membrane properties of the saturated *N*-palmitoyl-IPC (P-IPC) in one component bilayers as well as in complex bilayers together with 1-palmitoyl-2-oleoyl-*sn*-glycero-3-phosphocholine and cholesterol. The membrane properties of P-IPC were shown to be affected by calcium. According to anisotropy changes reported by DPH, the gel-to-liquid transition temperature (T_m) of P-IPC was 48 °C. Addition of 5 mM $CaCl_2$ during vesicle preparation markedly increased the T_m (65 °C). According to fluorescence quenching experiments in complex lipid mixtures, P-IPC formed sterol containing domains in an otherwise fluid environment. The P-IPC containing domains melted at a lower temperature and appeared to contain less sterol as compared to domains containing *N*-palmitoyl-sphingomyelin. Calcium further reduced the sterol content of the ordered domains and also increased the thermal stability of the domains. Calcium also induced vesicle aggregation of unilamellar vesicles containing P-IPC, as was observed by 4D confocal microscopy and dynamic light scattering. We believe that IPCs and the calcium induced effects could be important in numerous membrane associated cellular processes such as membrane fusion and in membrane raft linked processes.

1. Introduction

Inositol phosphorylceramides (IPCs) are a class of anionic sphingolipids with a single inositol-phosphate head group coupled to ceramide (Fig. 1) [1]. IPCs were initially identified as yeast sphingolipids in *Saccharomyces cerevisiae* and have later been identified in other yeasts, protozoa and plants [1–7]. IPCs are synthesized by transfer of the phosphoinositol moiety from phosphatidylinostol to the C-1-hydroxy group in ceramide by the enzyme, IPC synthase in the Golgi apparatus [8–10]. IPCs can further be modified through different biosynthetic pathways forming glycoinositol phosphorylceramides. In yeast, glycoinositol phosphorylceramides are formed by the addition of mannose to IPC forming mannose inositolphosphorylceramide and a further addition of inositol-phosphate forming mannose di(inositolphosphoryl)ceramide [2]. In plants and protozoa more complex glycoinositol phosphorylceramides, containing additional sugar groups can be formed [4,7]. In a recent quantitative shotgun masspectrometry study, inositol containing sphingolipids were shown to constitute about 13 mol% of the entire lipidome of *S. cerevisiae* [11]. Mannose di(inositolphosphoryl) ceramide was shown to be most abundant, constituting 10 mol% of the lipidome and IPC and mannose inositolphosphorylceramide constituting 1 and 2 mol% respectively [11]. Even though IPCs are present at low levels in *S. cerevisiae*, the local concentration of IPCs can be markedly increased through enrichment in lipid rafts. IPCs have been identified at higher concentrations in detergent resistant membranes in yeast and in *Leishmania (Viannia) braziliensis* [6,12]. The levels of IPC have also been shown to be markedly higher in specific secretory vesicles in *S. cerevisiae* [13]. In post-Golgi secretory vesicles destined for the plasma membrane the amount of IPC was doubled to about 4.5 mol% of the vesicle lipidome as compared to the lipidome of the trans-Golgi network/endosome system [13]. In mammals IPCs and glycoinositol phosphorylceramides have not been identified and in contrast to yeasts, a phosphocholine head group can be transferred from phosphatidylcholine to the C-1 hydroxy in ceramide, forming sphingomyelin [14]. Due to the apparent distinctions between sphingolipid biosynthetic pathways in fungi/protozoa and mammals, recent antifungal and anti-protozoal studies have focused on the IPC

Abbreviations: 7SLPC, 1-palmitoyl-2-stearoyl-(7-doxyl)-*sn*-glycero-3-phosphocholine; CTL, cholesta-5,7,9(11)-trien-3-beta-ol; DPH, 1,6-diphenyl-1,3,5-hexatriene; DPPG, 1,2-dipalmitoyl-*sn*-glycero-3-phosphoglycerol; IPC, inositol-phosphorylceramide; PI, L-α-phosphatidylinostol (Liver, Bovine); P-IPC, D-erythro-*N*-palmitoyl-inositol-phosphorylceramide; POPC, 1-palmitoyl-2-oleoyl-*sn*-glycero-3-phosphocholine; PSM, D-*erythro*-*N*-palmitoyl-sphingomyelin; T_m, transition temperature between gel and fluid phases

* Corresponding author. Tel.: +358 400 822164; fax: +358 2 215 4745.
E-mail address: anders.bjorkbom@abo.fi (A. Björkbom).

0005-2736/$ – see front matter © 2009 Elsevier B.V. All rights reserved.
doi:10.1016/j.bbamem.2009.11.003

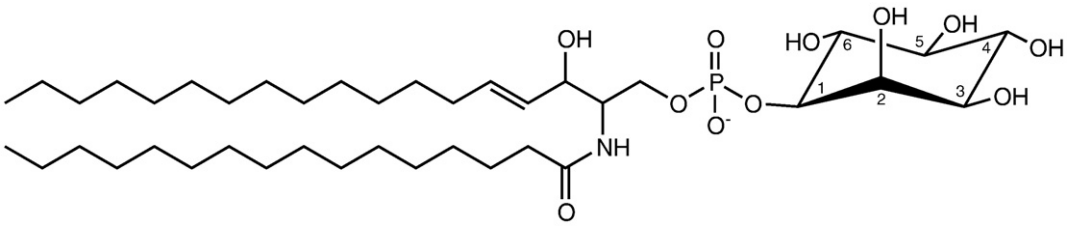

Fig. 1. Chemical structure of D-*erythro*-*N*-palmitoyl-inositol phosphorylceramide (P-IPC).

synthase as a potential drug target [15–18]. Natural compounds (and their derivatives) directed at the IPC-synthase (Aureobasidin A, Khafrefungin and Galbonolide A) have been shown to have inhibitory and antifungal activity [16,19].

Calcium and other multivalent cations have been shown to affect the phase behavior of phospholipids and to induce aggregation and fusion of vesicles containing anionic phospholipids [20,21]. Membrane fusion is an important step in many biological processes such as exocytosis, endocytosis and intracellular vesicular transport and is considered a multistep process involving membrane lipids and membrane proteins [22–24]. Calcium has also been shown to be involved in the regulation of IPC-mannosyl transferase in yeasts [25–27]. IPC-mannosyl transferase is responsible for the conversion of IPC to mannose-IPC and increased levels of calcium in the growth medium of yeast cells has been shown to increase the conversion of IPC to mannose-IPC [27]. Mutations in the genes encoding IPC-mannosyl transferases have also been shown to give calcium sensitive growth phenotypes [25]. An increase in calcium levels thus affects the sphingolipid composition by reducing the levels of IPC and increasing the levels of mannose-inositol phosphorylceramide and if IPC-mannosyl transferase activity is decreased, high calcium levels affect cell growth. IPC and calcium interactions have also been suggested to alter properties of ordered lipid domains, resulting in effects on signaling pathways [27].

Lipid rafts have been identified in the plasma membrane of yeasts and protozoa and IPCs have been identified as a constituent of lipid rafts in yeasts and protozoa through detergent extraction [6,12]. To study the formation of ordered domains containing P-IPC in model systems, we used a previously developed fluorescence quenching assay [28]. The most common long chain bases of sphingolipids in yeast are phytosphingosine and dihydrosphingosine whereas mammalian sphingolipids mostly contain the long chain base sphingosine [14]. The most abundant long chain base of IPC in *S. cerevisiae* was shown to be 18:0-phytosphingosine and in the protozoa *Leishmania major* the most abundant long chain base was shown to be 16:1-sphingosine, but also 16:0-phytosphingosine and 18:1-sphingosine long chain bases were identified [3,11]. The *N*-linked fatty acid moieties of IPCs in *S. cerevisiae* are usually long saturated fatty acids having 24–26 carbons, but shorter saturated fatty acids (14–18 carbons) have also been identified in *L. (Viannia) braziliensis* and *L. major* [3,6,11]. The saturated acyl chains of IPCs in *S. cerevisiae* can also be hydroxylated at one or two positions [11,13]. The IPC examined in this study was D-*erythro*-*N*-palmitoyl-IPC (P-IPC) containing the long chain base 18:1-sphingosine and 16:0 (palmitic acid) in the *N*-linked position. The sphingosine base and palmitic acid were chosen to facilitate comparison to the well characterized D-*erythro*-*N*-palmitoyl-sphingomyelin (PSM), assuring that differences in membrane properties arise only from differences in the head group structure. Cholesterol interactions with PSM and other sphingolipids have been thoroughly studied and using a structurally identical system, save for the head group structure of P-IPC, it can be assured that differences arise only from the properties of the head groups [28–30]. Since yeasts do not contain sphingomyelin it could also be speculated that IPCs and glycoinositol phosphorylceramides have similar functions in yeasts as sphingomyelins have in mammals. Therefore a direct comparison is warranted.

Acyl chain specific IPCs have, to our knowledge, not previously been studied in model systems and the objective of this study was to examine the membrane properties of P-IPC and compare them to the membrane properties of PSM. P-IPC was studied in pure and complex lipid model systems and the impact of calcium on the membrane properties of P-IPC was also assessed. Using a fluorescence quenching assay, P-IPC was shown to form sterol containing domains but with less sterol as compared to PSM containing domains. The ordered domains melted at higher temperatures in the presence of calcium and additionally the sterol content of the ordered domains was reduced. Calcium also induced aggregation of P-IPC containing vesicles as observed with 4D confocal microscopy and dynamic light scattering.

2. Materials and methods

2.1. Materials

1-palmitoyl-2-oleoyl-*sn*-glycero-3-phosphocholine (POPC), 1,2-dihexadecanoyl-*sn*-glycero-3-phospho-(1'-*rac*-glycerol) (DPPG), Rhodamine-phosphoethanolamine, bovine liver L-α-phosphatidylinositol (PI) and egg yolk sphingomyelin were from Avanti Polar Lipids inc. (Alabaster, AL, USA). Cholesterol was purchased from Sigma Chemicals Co. (St. Louis, MO, USA) and 1,6-diphenyl-3,5-hexatriene was from Molecular Probes (Leiden, The Netherlands). D-*erythro*-*N*-palmitoyl-sphingomyelin was purified from egg yolk sphingomyelin through reverse-phase HPLC (Supelco Discovery C-18 column, 25 cm × 21.2 mm, 5 μm particle size) using 100% methanol as mobile phase. The purity and identity of PSM was verified on a Micromass Quattro II mass spectrometer. Cholesta-5,7,9(11)-trien-3-beta-ol (CTL) was synthesized using the method described in [31]. CTL was purified using reverse-phase HPLC (Supelco Discovery C-18 column, 25 cm × 21.2 mm, 5 μm particle size) with 95% methanol and 5% hexane as mobile phase. 1-Palmitoyl-2-stearoyl-(7-doxyl)-*sn*-glycero-3-phosphocholine (7SLPC) was synthesized from (7-doxyl)-stearic acid (TCI Europe N.V., Belgium) and 1-palmitoyl-2-hydroxy-*sn*-glycero-3-phosphocholine according to [32]. 7SLPC was purified using reverse-phase HPLC (Supelco Discovery C-18 column, 25 cm × 21.2 mm, 5 μm particle size) with 100% methanol as mobile phase. The purity and identity of 7SLPC was confirmed on a Micromass Quattro II mass spectrometer. CTL and 7SLPC were stored at −87 °C in the dark in an argon environment. Before use CTL was dissolved in argon purged ethanol and 7SLPC was dissolved in argon purged hexane/2-propanol, (2:3, by vol) and used within 3 days. Stock solutions of all lipids were stored at - 20 °C in the dark and before use the stock solutions were taken to ambient temperature. The H_2O used was purified with a Millipore UF Plus purification system, giving a product with an 18.2 MΩ cm resistivity.

2.2. Synthesis of P-IPC

D-erythro-*N*-palmitoyl-inositol-phosphorylceramide was synthesized from 3.7 μmol D-*erythro*-sphingosyl phosphoinositol (Avanti

Polar Lipids inc.) and 37 μmol palmitic anhydride (Sigma, St. Louis, MO, USA). The compounds were dried in vacuum for 1 h and dissolved in 500 μl dry dichloromethane/methanol (7:3, by vol). 5 μl triethylamine (Fluka Chemie GmbH, Buchs, Switzerland) was added to the reaction mixture and the reaction vial was flushed with argon and sealed and left on stirring at 23–30 °C for 12–17 h. The reaction mixture was dried with nitrogen and redissolved in chloroform/methanol (2:1, by vol) for purification. The redissolved mixture was purified with solid phase extraction on a Mega Bond Elut NH2 straight barrel column (1 g, 6 ml) with 40 μm particle size and aminopropyl as the bonded functional group (Varian inc., Palo Alto, CA, USA). The column was eluted with (1) chloroform/isopropanol (2:1, by vol); (2) diethyl ether with 2 vol% acetic acid; (3) methanol and (4) chloroform/methanol/4,2 M NH_3 (9:7:2, by vol). Fraction 4 was neutralized with acetic acid and extracted with butanol. The butanol phase was dried with nitrogen and redissolved in methanol for purification on normal phase HPLC (Supelco Supelcosil LC-SI column, 25 cm × 10 mm, 5 μm particle size). The mobile phase was chloroform/methanol/mQ-H_20 (55:39:6, by vol) and the purity and identity of P-IPC was verified with a Micromass Quattro II mass spectrometer.

2.3. Preparation of vesicles

Lipid and fluorescent probe solutions were taken to ambient temperature and mixed in desired proportions in glass tubes. The lipid and probe solutions were dried under a stream of nitrogen at 40 °C followed by additional drying in vacuum. The lipid mixtures were heated above the transition temperature between gel and fluid phases (T_m) of the highest melting lipid component, and buffer of same temperature was added to the lipid mixtures. The lipid/buffer dispersion was kept at a temperature exceeding the T_m of the highest melting lipid for at least 30 min, followed by either sonication or the extrusion procedure. Probe sonication was performed for 2 min, also above the highest T_m, using a Branson probe sonifier W-450 (25% duty cycle, power output 10 W (Branson Ultrasonics, Danbury, CT, USA)) to form multilamellar vesicles. For preparation of unilamellar vesicles the lipid/buffer dispersions were bath sonicated for 10 min, again above the highest T_m, using a Branson bath sonicator 2510 (Branson Ultrasonics) followed by the extrusion procedure (Avanti mini extruder using 0.2 μm polycarbonate membranes filter) at the same temperature. The lipid solution was extruded 11 times through the polycarbonate filter. Buffers consisted of 50 mM Tris (MP Biomedicals LLC, Solon, OH, USA) pH 7.4 with 140 mM NaCl either with or without 5 mM $CaCl_2$. For the aggregation experiments Tris buffer with 50 mM $CaCl_2$ was added to the calcium-free buffer to adjust the final $CaCl_2$ concentration to 5 mM.

2.4. Steady-state fluorescence anisotropy measurements

The steady-state anisotropy of DPH was measured on a Quanta Master spectrofluorimeter operating in the T-format (Photon Technology International, Lawrenceville, NJ, USA). DPH was excited at 360 nm and the emission intensity was measured at 430 nm with slits at 5 nm, magnetic stirring and a temperature scan rate of 5 °C/min. The lipid concentration was 50 μM and the probe concentration was 1 mol%. The transition temperatures given were obtained by visual assessment and the graphs shown are representative of several experiments. The anisotropy was calculated as described in [33].

2.5. Fluorescence quenching measurements

The fluorescence quenching measurements were performed on a Quanta Master spectrofluorimeter operating in the L-format (Photon Technology International) according to the method outlined in Ref. [28]. The fluorescence quenching assay is based on the separation of the fluorescent reporter molecule from the quencher 7SLPC in the presence of ordered domains in the model systems. CTL is a fluorescent sterol analogue and was used to identify sterol containing ordered domains. DPH is a fluorescent reporter molecule partitioning more equally between ordered and disordered phases and was used to identify ordered domains, regardless of the presence of sterol. CTL is thus used to study ordered domains containing sterol and DPH is used to study ordered domains in general, not necessarily containing sterol. The results from the fluorescence quenching assay are shown as the ratio between the *F*-sample and the F_0-sample. Only the *F*-sample contains the quencher so the F/F_0 ratio gives the relative amount of unquenched fluorescence, and when this is plotted as a function of temperature the melting of ordered domains can be seen as a decrease in the F/F_0 ratio. The amount of CTL, and thus the amount of sterol molecules in the ordered domains, can be assessed from the amplitude of the melting of the ordered domains. The amplitude is proportional to the amount of CTL that is protected from quenching by 7SLPC. The higher the amplitude, the higher the amount of CTL and thus sterol in the ordered domains. The samples consisted of 60 mol% POPC, 10 mol% of cholesterol and 30 mol% of either PSM or P-IPC. In the *F*-sample 7SLPC replaced 50 mol% of POPC. For CTL and DPH the excitation and emission wavelengths were 324/374 nm and 360/430 nm, respectively. The quenching experiments were performed using 5 nm slits, magnetic stirring and a temperature scan rate of 5 °C/min. The lipid concentration was 100 μM and the probe concentration was 1 mol%. The graphs shown are representative of several experiments.

2.6. Confocal microscopy and data analysis of the microscopic data

The 4D (4-dimensional; 3 spatial dimensions and time) laser scanning confocal microscopy experiments were performed with an AxioObserver Z1 (63×/1.4 objective) equipped with LSM510 (Carl Zeiss Inc., Jena, Germany). Data analysis and visualizations were performed using the open source software BioImageXD [34]. Cluster sizes were calculated using thresholding-based segmentation and connected component labeling and visualized as 3D ray casting volume renderings. The experiments were performed at 21 ± 1 °C using unilamellar vesicles in Tris buffer. 50 mM $CaCl_2$ containing Tris buffer was added to the samples to a final concentration of 5 mM (total sample volume 200 μl) and for controls calcium-free Tris buffer was added. The figures shown are representative of several experiments.

2.7. Dynamic light scattering measurements

Dynamic light scattering experiments were performed on a Malvern Zetasizer Nano-S (Malvern Instruments Ltd, Worcestershire, UK). The experiments were performed at 21 °C using 100 μM unilamellar vesicle solutions in Tris buffer. 50 mM $CaCl_2$ containing Tris buffer was added to the samples to a final concentration of 5 mM (total sample volume 200 μl) and for controls calcium-free Tris buffer was added. The Zetasizer Nano-S was equipped with a 633 nm laser and operating at a backscattering angle of 173°. The results are given as mean *Z*-average (nm) size calculated from the dynamic light scattering intensity for several experiments. The *Z*-average is the size value calculated with cumulant analysis of the autocorrelation functions. Given the nature of the *z*-average and the aggregation process the *z*-average values can only be used for internal comparison using the same experimental setup and technique.

3. Results

3.1. Membrane order in P-IPC containing vesicles

Membrane order and T_m were determined by performing steady-state DPH-anisotropy as a function of temperature (Fig. 2). The DPH molecule is positioned in the inner, acyl chain region of the lipid bilayer [35,36]. A

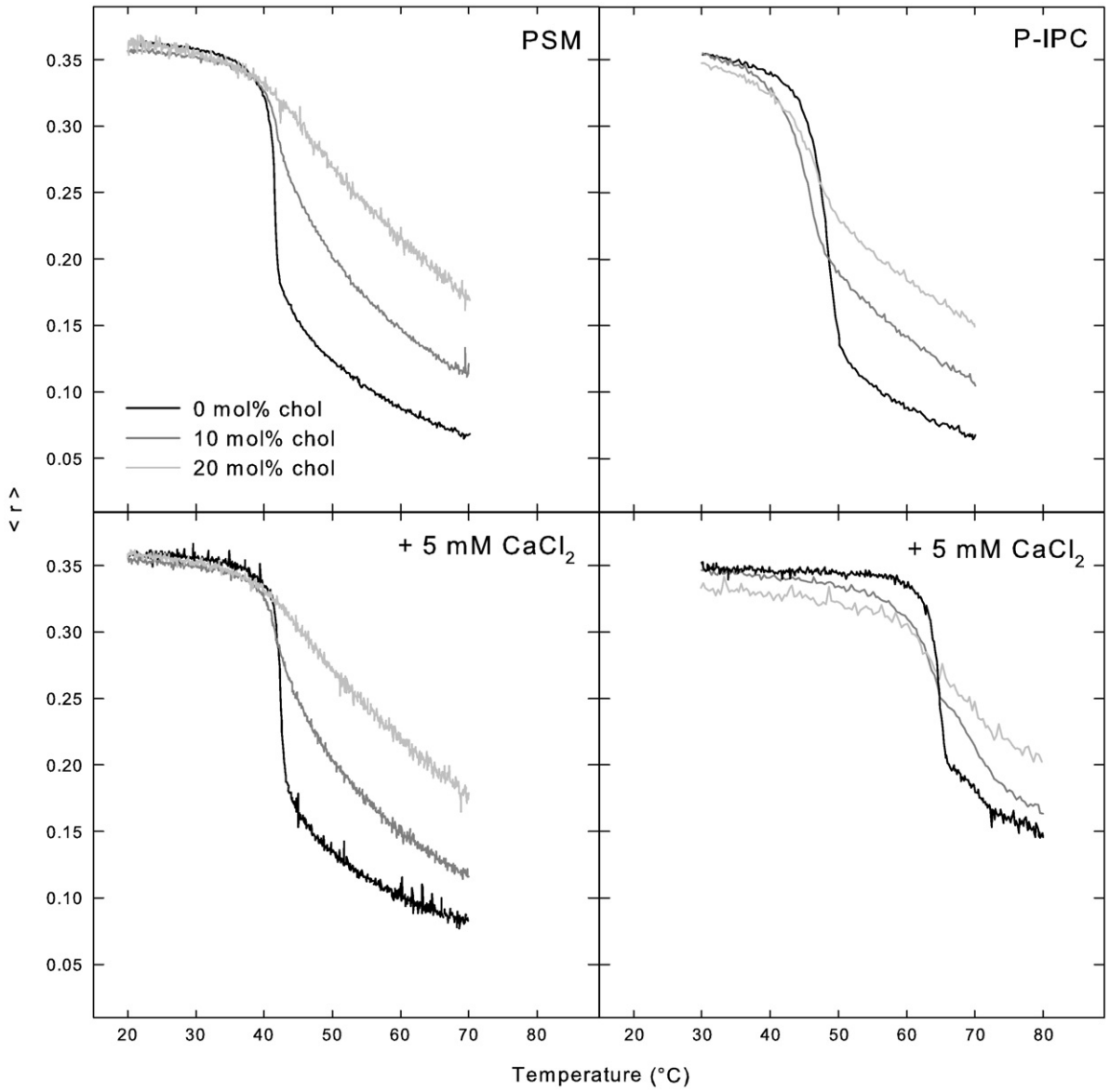

Fig. 2. Anisotropy of DPH in vesicles containing either pure P-IPC or PSM and in mixtures with 10 and 20 mol% cholesterol. The anisotropy is plotted as a function of temperature for vesicles containing sphingolipid (black line), 10 mol% cholesterol (dark grey line) and 20 mol% cholesterol (grey line). The upper panels show the anisotropy experiments performed in Tris buffer and the lower panels show the anisotropy experiments performed in Tris buffer containing 5 mM $CaCl_2$. The experiments were performed with multilamellar bilayer vesicles with 1 mol% DPH and the scan rate was 5 °C/min. The graphs are representative of several experiments.

higher degree of order for the acyl chains will result in a higher anisotropy for DPH since the possibilities for movement of the DPH molecule are reduced [35,37]. The T_m of pure P-IPC vesicles was 47.8 ± 0.4 °C in Tris buffer and when calcium was included, during vesicle preparation, the T_m increased to 64.8 ± 0.2 °C. Calcium had a large effect on the T_m of P-IPC whereas a small effect was observed on the T_m for pure PSM vesicles (from 41.9 ± 0.3 to 42.5 ± 0.3 °C). The T_m of PSM in calcium-free Tris buffer correlates with previous studies [38]. Inclusion of calcium to the Tris buffer also increased the anisotropy of DPH in the fluid phase for P-IPC containing vesicles, whereas the anisotropy in the fluid phase for PSM containing vesicles was unaffected.

Cholesterol has an ordering and condensing effect on the acyl chains of liquid crystalline phospholipids [39]. 10 and 20 mol% of cholesterol had a similar ordering effect on the acyl chains of P-IPC and PSM containing vesicles above T_m, when experiments where performed in calcium-free Tris buffer. In calcium containing Tris buffer the DPH anisotropy in pure P-IPC vesicles above T_m was increased and the relative effect of cholesterol on the acyl chain order was decreased as compared to the situation in calcium-free Tris buffer. For PSM the ordering effect of cholesterol above T_m was very similar regardless of the presence of calcium.

3.2. Formation of ordered domains containing P-IPC

The domain formation was assessed using a fluorescence quenching assay with either CTL or DPH as the fluorescent reporter molecule together with the quencher 7SLPC [28]. Cholesterol was used as the sterol component in this study, since we wanted to compare the membrane properties of IPCs to sphingomyelin and most studies examining the membrane properties of sphingomyelin have been performed with cholesterol. Ergosterol was, however, also tested as the sterol component in the fluorescence quenching assay as mentioned later. The fluorescent cholesterol analogue CTL was used to observe the formation of sterol containing domains and DPH was used to observe ordered domains in general (not necessarily containing high levels of cholesterol) [28,40,41]. As observed from the decrease in the F/F_0 ratio (indicated by arrow) P-IPC was shown to form ordered domains in an otherwise fluid environment (Fig. 3).

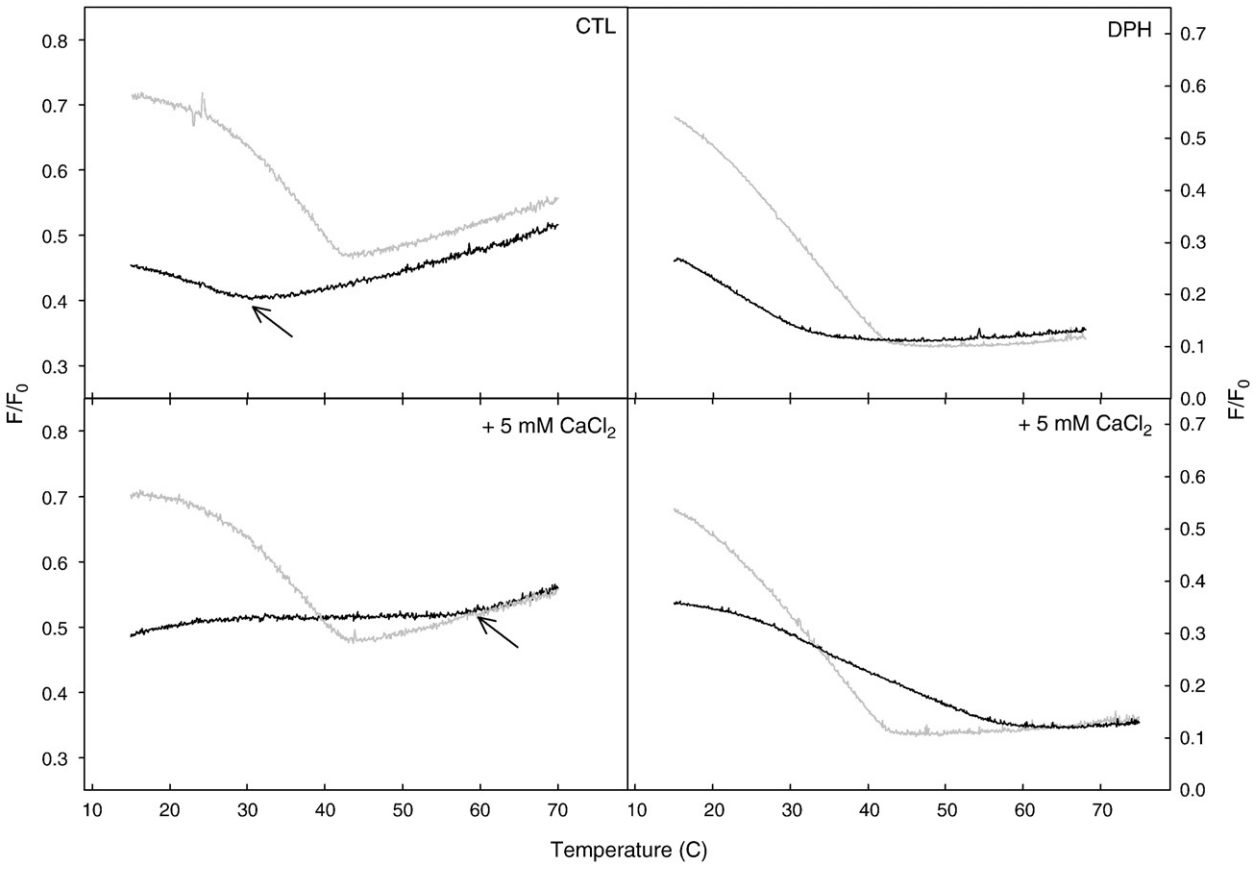

Fig. 3. Thermal stability of ordered domains in an otherwise fluid environment as measured by fluorescence quenching. Fluorescence quenching of CTL (left panels) or DPH (right panels) in multicomponent vesicles containing P-IPC (black) or PSM (gray) as the domain forming sphingolipid. To assess the formation and thermal stability of sterol containing ordered domains we used the fluorescent cholesterol analogue CTL and the quencher 7SLPC. To assess the formation and thermal stability of ordered domains in general (not necessarily containing cholesterol) we used DPH and the quencher 7SLPC. The sample composition was POPC/sphingolipid/cholesterol (60:30:10, molar ratio) with 1 mol% of CTL or DPH. In the *F*-sample, 7SLPC replaced 50% of POPC. Lower panels show experiments performed in the presence of 5 mM $CaCl_2$. The experiments were performed with multilamellar bilayer vesicles at a scan rate of 5 °C/min. The graphs are shown as the F/F_0 ratio versus temperature and the graphs are representative of several experiments. Arrows show the melting of P-IPC containing ordered domains.

P-IPC formed ordered domains containing less sterol as compared to ordered domains with PSM as the domain forming sphingolipid (Fig. 3, upper left panel). The relative amount of sterol in the domains can be assessed from the amplitude of the F/F_0-curve. Ordered domains containing P-IPC also melted at a lower temperature as compared to domains with PSM. The melting of ordered domains containing P-IPC was complete at about 30 °C and ordered domains with PSM were fully melted at about 41 °C. The quenching of DPH (Fig. 3, upper right panel) reported on P-IPC containing domains with a similar thermal stability as the fluorescence quenching experiments with CTL. Melting of the ordered domains was finished at approximately 30 °C. The domain forming properties of P-IPC together with ergosterol was also assessed using the same fluorescence quenching assay but with dehydroergosterol as the fluorescent reporter molecule. The results were similar to the fluorescence quenching studies with cholesterol and CTL. P-IPC formed sterol containing domains together with ergosterol but with an increase in thermal stability as compared to domains with cholesterol (data not shown). These findings are consistent with a previous study showing that both cholesterol and ergosterol formed ordered domains with sphingolipids, and that ergosterol containing domains melted at higher temperatures as compared to cholesterol containing domains [42].

3.3. Calcium effects on the formation of ordered domains containing P-IPC

The formation and properties of ordered domains containing P-IPC was affected by the presence of calcium (Fig. 3, lower panels). Fluorescence quenching of CTL (Fig. 3, lower left panel) showed that thermally more stable sterol containing domains were formed when calcium was included in the Tris buffer during vesicle preparation. Calcium also seemed to decrease the amount of sterol in the ordered domains. The relative sterol content in the domains can be determined from the amplitude of the F/F_0-curve. Fluorescence quenching of DPH (Fig. 3, lower right panel) also showed that ordered domains were formed in the presence of calcium and that the ordered domains were completely melted at a markedly higher temperature in the presence of calcium. The melting of ordered domains containing PSM was not significantly affected by calcium.

3.4. Calcium induced aggregation of P-IPC containing unilamellar vesicles

Using laser scanning confocal microscopy (Fig. 4) and dynamic light scattering experiments (Fig. 5), calcium was shown to induce aggregation of vesicles containing P-IPC. In the microscopy experiments calcium was added to unilamellar vesicles composed of PSM:P-IPC (1:1, molar ratio) to a final concentration of 5 mM. Immediately after addition of calcium the mean volume of the vesicle aggregates increased about 6 times and after 60 min the volume had increased about 60 times (Fig. 4, upper panels). When buffer lacking calcium was added to the unilamellar vesicles no aggregation was observed (Fig. 4, lower panels). The aggregation was studied as a time-series and aggregation was also observed when the samples had been kept in the dark until images were acquired. This procedure excludes possible artifacts induced by the microscope, such as light induced aggregation.

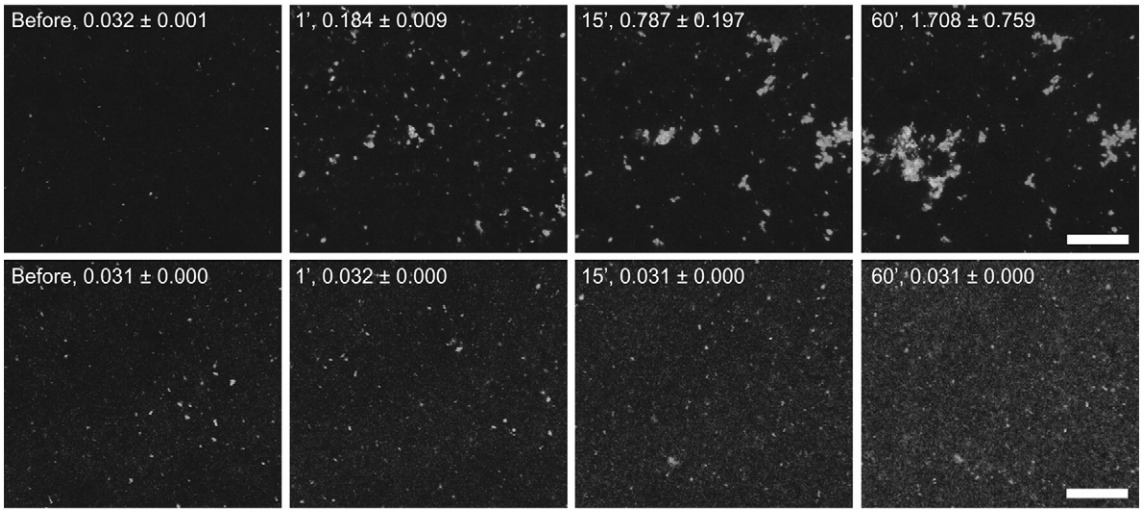

Fig. 4. Calcium induced aggregation of vesicles containing P-IPC. 4D Confocal microscopy was used to study aggregation of unilamellar vesicles composed of P-IPC:PSM (1:1, molar ratio) at 21 ± 1 °C. The upper panels show the aggregation after addition of $CaCl_2$ to a final concentration of 5 mM and the lower panels are controls with calcium-free Tris buffer. The time points for the images, as indicated in the upper left corner of each panel, are taken immediately before and after addition of calcium and 15 min and 60 min after the addition. The average sizes of vesicles/aggregates are given in μm^3 in the upper left corner of each panel. Bars, 10 μm.

Dynamic light scattering was used to study the aggregation of vesicles composed of PSM or equimolar mixtures of PSM and P-IPC, DPPG or bovine liver PI (Fig. 5). PI was studied to enable comparison to a glycerol-based inositol containing lipid and DPPG for comparison to a negatively charged membrane lipid. Vesicles composed of pure PSM did not show aggregation in the presence of calcium, whereas vesicles containing P-IPC, PI or DPPG showed aggregation. The increase in aggregate size for DPPG containing vesicles was markedly smaller as compared to vesicles containing either P-IPC or PI. The calcium was added as 50 mM $CaCl_2$ dissolved in Tris buffer and when calcium-free Tris buffer was added no aggregation was observed for any of the lipid compositions examined.

4. Discussion

In this study we report on the membrane properties of the non-mammalian sphingolipid P-IPC in pure and complex model membranes containing POPC and cholesterol. The properties of P-IPC have been compared to the well characterized and acyl chain matched membrane sphingolipid PSM [28,43–45]. The phase behavior and properties of membrane lipids have been shown to be affected by inorganic cations and we have studied the effects of the biologically highly significant calcium ion on the membrane properties of P-IPC.

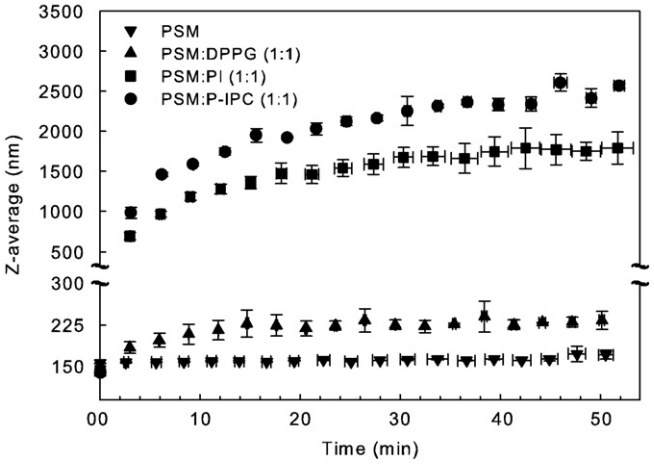

Fig. 5. Calcium induced vesicle aggregation studied with dynamic light scattering. Aggregation of pure PSM (▼) and equimolar mixtures of PSM and DPPG (▲), PI (■) and P-IPC (●) unilamellar vesicles in Tris buffer after addition of $CaCl_2$ to final concentration of 5 mM at 21 °C. The results are given as the mean *Z*-average (nm) as a function of time after addition of calcium for several reproducible experiments.

Pure P-IPC multilamellar bilayer vesicles have a higher T_m as compared to bilayers containing the acyl chain matched sphingolipid PSM (47.8 ± 0.4 °C and 41.9 ± 0.3 °C, respectively). PSM and P-IPC are identical in the ceramide moiety so differences in membrane properties arise from differences in the structure of the head groups linked to the hydroxyl group of palmitoyl-ceramide. The inositol head group (Fig. 1) contains hydroxyl groups which can act as donors and acceptors in intra- and intermolecular hydrogen bonding [46,47]. Compared to the zwitterionic PSM molecules, electrostatic interactions between the anionic P-IPC molecules could be expected to cause molecular repulsion giving rise to destabilization of molecular interactions and a lower T_m for P-IPC bilayers. However, the DPH data indicated that interactions between the P-IPC molecules were stronger as compared to interactions between PSM molecules in one component systems. The higher T_m for P-IPC bilayers could be explained by stronger interactions between the hydroxyl groups in the inositol head groups due to hydrogen bonding taking precedence over the electrostatic repulsion between the negatively charged phosphate moieties. The conformation of the inositol group as compared to the choline group could also affect lipid interactions. The inositol group has been shown to be positioned parallel to the bilayer normal as compared to the phosphocholine group which lies more or less parallel to the bilayer surface [47,48]. The conformation of the inositol head group could thus allow closer contact between the P-IPC molecules and increase acyl chain interactions, resulting in a higher T_m. The closer contact of the acyl chains could also explain the lower amount of sterol in P-IPC containing ordered domains as compared to PSM containing ordered domains. The properties of the inositol head group and the levels of P-IPC used in the DPH experiments, could possibly induce the formation of inverted hexagonal phase or other phase states. However, using DPH anisotropy we only observed one transition corresponding to the acyl chain melting transition (no detection of lamellar to nonlamellar phase). Dynamic light scattering experiments on P-IPC containing vesicles also showed that we were able to prepare stable and uniform vesicles through the extrusion procedure (data not shown). When calcium was present in the buffer the situation was, however, markedly different.

Calcium affected the membrane properties of P-IPC both laterally in the membrane and macroscopically between unilamellar bilayer vesicles resulting in increased melting temperature and vesicle aggregation. Inorganic cations have been shown to have large effects on the phase behavior of membrane lipids (for reviews, see [20,49–51]) and also to induce vesicle aggregation or fusion of vesicles [21,23,52–55]. The calcium levels used in this study are quite high compared to physiological conditions. Calcium concentrations can, however, locally be markedly higher as compared to the low resting cytosolic calcium levels [56]. Excess calcium levels have also previously been used in similar model system studies [57–59]. When calcium was added to the buffer, before formation of multilamellar bilayer vesicles, the T_m of pure P-IPC vesicles was increased by 17 °C and the T_m of PSM vesicles by 0.6 °C as reported by the anisotropy of DPH. Effects of calcium on the phase behavior of sphingomyelin (bovine brain) have previously been studied using infrared spectroscopy [60]. Calcium was shown to dehydrate the phosphate moiety and increase the interfacial H-bonding resulting, as in our study, in an slightly increased T_m [60]. Calcium affects the phase behavior of membrane lipids through a multitude of interactions depending on the structure and charge of the interface and the head group. Calcium interactions can roughly be categorized as indirect effects on the hydration shell of the lipid aggregates and direct interactions with the lipid aggregates [20]. Calcium increases the transition temperature of negatively charged phosphatidylserines through the formation of complexes with the phosphate group. The complex formation decreases the degree of hydration and changes the conformation of the phosphate group, resulting in an increased transition temperature [20]. For P-IPC we propose a similar complex formation between calcium and the phosphate group resulting in charge neutralization and a closer contact between the P-IPC molecules. The closer proximity of the molecules could also increase the hydrogen bonding, not only between the ceramide moieties at the interface, but also between the inositol groups explaining the increase in T_m. The membrane order in the fluid phase for pure P-IPC vesicles with calcium was also higher as compared to the order in P-IPC vesicles lacking calcium. The increased order in the fluid phase could be explained by stronger interactions between the P-IPC head groups in the fluid phase. A similar increased order in the fluid phase due to calcium interactions has been shown for dipalmitoylphosphatidic acid using Raman spectroscopy [57].

In addition to increasing the T_m of P-IPC bilayers, calcium induced aggregation of P-IPC containing vesicles. The formation of local packing defects at the boundaries of calcium induced lateral domains could induce the formation of energetically more favorable lipid aggregates, leading to the observed aggregation [54]. As seen in the fluorescence quenching assay, calcium was able to affect interactions between P-IPC molecules and enhance or induce the formation of P-IPC containing ordered domains. At the domain boundaries local packing defects could appear and upon contact between the domain boundaries energetically more favorable lipid aggregates could be formed. Calcium-induced dehydration of the lipid interfaces could also account for the observed aggregation by allowing vesicles to come in much closer proximity of each other, and thus induce aggregation [52]. Induction of membrane curvature could also lead to the formation of inverse hexagonal and inverse micellar cubic phases causing aggregation. Formation of curved membrane interfaces have previously been shown for glycerol based phosphatidylinositoles under limited hydration conditions [61]. Calcium could thus induce aggregation by binding to the P-IPC molecules causing packing defects, dehydrating the membrane interface and/or inducing curved membrane interfaces.

IPCs have been identified in detergent resistant membranes in *L. (Viannia) braziliensis* and *S. cerevisiae* and we found that P-IPC was able to form sterol containing ordered domains in model systems [6,12]. Cholesterol was used as the sterol component in this study since cholesterol interactions with PSM and other sphingolipids are thoroughly documented in the literature [28,62,63]. The objective of the study was to characterize the membrane properties of P-IPC and to compare how the inositol head group affected membrane properties, as compared to the phosphocholine head group in PSM. To facilitate the comparison we used an identical model system for the study of both P-IPC and PSM, containing cholesterol. The DPH experiments in binary systems showed that cholesterol interacts with P-IPC and that cholesterol was able to increase the order of the acyl chains. In ternary systems cholesterol has increased partitioning possibilities and using a fluorescence quenching assay we showed that P-IPC was able to interact with cholesterol and form sterol containing domains and that the domains were thermally more stable if calcium was present (Fig. 3). Calcium has previously been shown to increase the melting temperature of ordered domains containing the negatively charged glycosphingolipid *N*-palmitoyl-sulfatide [58]. The same explanations, as mentioned above for P-IPC/calcium interactions in pure and binary systems, can also be applied to the ternary systems used here. Calcium increased the interactions between the P-IPC molecules and the stronger interactions even appeared to decrease the amount of sterol in the ordered domains. The DPH quenching data clearly showed a thermal stabilization of ordered domains in the presence of calcium. The stabilization correlates well with the calcium induced increase in T_m, observed with the anisotropy of DPH in pure P-IPC systems (Fig. 2).

In conclusion, we showed that P-IPC was able to form sterol containing ordered domains in model systems and that the phase behavior of P-IPC was markedly affected by calcium. Calcium increased the melting temperature of P-IPC containing domains and induced aggregation of P-IPC containing vesicles. Using sphingolipids only differing in the head group region we showed that the calcium-induced effects arose from interactions with the inositol head group. IPCs, mannose inositolphosphorylceramides and mannose di(inositolphosphoryl)ceramides constitute the major sphingolipid species in *S. cerevisiae* [11]. Future prospects would be to analyze the membrane properties of IPCs and mannosylated IPCs in yeast like systems, to better understand the membrane functions and interplay between these highly abundant membrane lipids.

Acknowledgements

The authors wish to thank Stina Maunula for initial experiments and acknowledge financial support from the National Graduate School in Informational and Structural Biology, Åbo Akademi University, The Academy of Finland, The Sigrid Juselius foundation, The Magnus Ehrnrooth foundation and the Medicinska understödsföreningen Liv och Hälsa r.f.

References

[1] S.W. Smith, R.L. Lester, Inositol phosphorylceramide, a novel substance and the chief member of a major group of yeast sphingolipids containing a single inositol phosphate, J. Biol. Chem. 249 (1974) 3395–3405.
[2] R.C. Dickson, R.L. Lester, Yeast sphingolipids, Biochim. Biophys. Acta 1426 (1999) 347–357.
[3] F.F. Hsu, J. Turk, K. Zhang, S.M. Beverley, Characterization of inositol phosphorylceramides from *Leishmania major* by tandem mass spectrometry with electrospray ionization, J. Am. Soc. Mass Spectrom. 18 (2007) 1591–1604.
[4] R.L. Lester, R.C. Dickson, Sphingolipids with inositolphosphate-containing head groups, Adv. Lipid Res. 26 (1993) 253–274.
[5] O. Lhomme, M. Bruneteau, C.E. Costello, P. Mas, P.M. Molot, A. Dell, P.R. Tiller, G. Michel, Structural investigations and biological activity of inositol sphingophospholipids from *Phytophthora capsici*, Eur. J. Biochem. 191 (1990) 203–209.
[6] K.A. Yoneyama, A.K. Tanaka, T.G. Silveira, H.K. Takahashi, A.H. Straus, Characterization of *Leishmania (Viannia) braziliensis* membrane microdomains, and their role in macrophage infectivity, J. Lipid Res. 47 (2006) 2171–2178.
[7] R.A. Laine, Phosphorous-containing glycosphingolipids, Chem. Phys. Lipids 42 (1986) 129–135.
[8] G.W. Becker, R.L. Lester, Biosynthesis of phosphoinositol-containing sphingolipids from phosphatidylinositol by a membrane preparation from *Saccharomyces cerevisiae*, J. Bacteriol. 142 (1980) 747–754.

[9] J.A. Hackett, P.J. Brennan, The isolation and biosynthesis of the ceramide-phosphoinositol of *Aspergillus niger*, FEBS Lett. 74 (1977) 259–263.
[10] T.P. Levine, C.A. Wiggins, S. Munro, Inositol phosphorylceramide synthase is located in the Golgi apparatus of *Saccharomyces cerevisiae*, Mol. Biol. Cell 11 (2000) 2267–2281.
[11] C.S. Ejsing, J.L. Sampaio, V. Surendranath, E. Duchoslav, K. Ekroos, R.W. Klemm, K. Simons, A. Shevchenko, Global analysis of the yeast lipidome by quantitative shotgun mass spectrometry, Proc. Natl. Acad. Sci. U. S. A. 106 (2009) 2136–2141.
[12] M. Bagnat, S. Keranen, A. Shevchenko, A. Shevchenko, K. Simons, Lipid rafts function in biosynthetic delivery of proteins to the cell surface in yeast, Proc. Natl. Acad. Sci. U. S. A. 97 (2000) 3254–3259.
[13] R.W. Klemm, C.S. Ejsing, M.A. Surma, H.J. Kaiser, M.J. Gerl, J.L. Sampaio, R.Q. de, C. Ferguson, T.J. Proszynski, A. Shevchenko, K. Simons, Segregation of sphingolipids and sterols during formation of secretory vesicles at the trans-Golgi network, J. Cell Biol. 185 (2009) 601–612.
[14] R.C. Dickson, Sphingolipid functions in *Saccharomyces cerevisiae*: comparison to mammals, Annu. Rev. Biochem. 67 (1998) 27–48.
[15] R.C. Dickson, Thematic review series: sphingolipids. New insights into sphingolipid metabolism and function in budding yeast,, J. Lipid Res. 49 (2008) 909–921.
[16] Y. Sugimoto, H. Sakoh, K. Yamada, IPC synthase as a useful target for antifungal drugs, Curr. Drug Targets Infect. Disord. 4 (2004) 311–322.
[17] P.W. Denny, H. Shams-Eldin, H.P. Price, D.F. Smith, R.T. Schwarz, The protozoan inositol phosphorylceramide synthase: a novel drug target that defines a new class of sphingolipid synthase, J. Biol. Chem. 281 (2006) 28200–28209.
[18] N.H. Georgopapadakou, Antifungals targeted to sphingolipid synthesis: focus on inositol phosphorylceramide synthase, Expert Opin. Investig. Drugs 9 (2000) 1787–1796.
[19] J.M. Fostel, P.A. Lartey, Emerging novel antifungal agents, Drug Discov. Today 5 (2000) 25–32.
[20] H. Hauser, Effect of inorganic cations on phase transitions, Chem. Phys. Lipids 57 (1991) 309–325.
[21] D. Papahadjopoulos, S. Nir, N. Duzgunes, Molecular mechanisms of calcium-induced membrane fusion, J. Bioenerg. Biomembr. 22 (1990) 157–179.
[22] K.L. Furber, M.A. Churchward, T.P. Rogasevskaia, J.R. Coorssen, Identifying critical components of native Ca2+-triggered membrane fusion. Integrating studies of proteins and lipids, Ann. N. Y. Acad. Sci. 1152 (2009) 121–134.
[23] D. Papahadjopoulos, G. Poste, Calcium-induced phase separation and fusion in phospholipid membranes, Biophys. J. 15 (1975) 945–948.
[24] W. Wickner, R. Schekman, Membrane fusion, Nat. Struct. Mol. Biol. 15 (2008) 658–664.
[25] T. Beeler, K. Gable, C. Zhao, T. Dunn, A novel protein, CSG2p, is required for Ca2+ regulation in *Saccharomyces cerevisiae*, J. Biol. Chem. 269 (1994) 7279–7284.
[26] S. Uemura, A. Kihara, J. Inokuchi, Y. Igarashi, Csg1p and newly identified Csh1p function in mannosylinositol phosphorylceramide synthesis by interacting with Csg2p, J. Biol. Chem. 278 (2003) 45049–45055.
[27] S. Uemura, A. Kihara, S. Iwaki, J. Inokuchi, Y. Igarashi, Regulation of the transport and protein levels of the inositol phosphorylceramide mannosyltransferases Csg1 and Csh1 by the Ca2+-binding protein Csg2, J. Biol. Chem. 282 (2007) 8613–8621.
[28] Y.J. Bjorkqvist, T.K. Nyholm, J.P. Slotte, B. Ramstedt, Domain formation and stability in complex lipid bilayers as reported by cholestatrienol, Biophys. J. 88 (2005) 4054–4063.
[29] J. Aittoniemi, P.S. Niemela, M.T. Hyvonen, M. Karttunen, I. Vattulainen, Insight into the putative specific interactions between cholesterol, sphingomyelin, and palmitoyl-oleoyl phosphatidylcholine, Biophys. J. 92 (2007) 1125–1137.
[30] S. Maunula, Y.J. Bjorkqvist, J.P. Slotte, B. Ramstedt, Differences in the domain forming properties of N-palmitoylated neutral glycosphingolipids in bilayer membranes, Biochim. Biophys. Acta 1768 (2007) 336–345.
[31] R.T. Fischer, F.A. Stephenson, A. Shafiee, F. Schroeder, delta 5,7,9(11)-Cholestatrien-3 beta-ol: a fluorescent cholesterol analogue, Chem Phys. Lipids 36 (1984) 1–14.
[32] R. Bittman, Chemical Preparation of Glycerolipids: a Review of Recent Syntheses, in: G. Cevec (Ed.), Phospholipids handbook, Marcel Dekker, Inc., 1993, pp. 154–155.
[33] J.R. Lakowicz, Principles of Fluorescence Spectroscopy, Springer Science +Business Media, LLC, New York, 2006.
[34] P. Kankaanpaa, K. Pahajoki, V. Marjomaki, J. Heino, D. White, BioImageXD software, www.bioimagexd.net, 2006.
[35] J.R. Lakowicz, F.G. Prendergast, D. Hogen, Differential polarized phase fluorometric investigations of diphenylhexatriene in lipid bilayers. Quantitation of hindered depolarizing rotations, Biochemistry 18 (1979) 508–519.
[36] R.D. Kaiser, E. London, Location of diphenylhexatriene (DPH) and its derivatives within membranes: comparison of different fluorescence quenching analyses of membrane depth, Biochemistry 37 (1998) 8180–8190.
[37] J.R. Lakowicz, F.G. Prendergast, D. Hogen, Fluorescence anisotropy measurements under oxygen quenching conditions as a method to quantify the depolarizing rotations of fluorophores. Application to diphenylhexatriene in isotropic solvents and in lipid bilayers, Biochemistry 18 (1979) 520–527.
[38] M. Kuikka, B. Ramstedt, H. Ohvo-Rekila, J. Tuuf, J.P. Slotte, Membrane properties of D-erythro-N-acyl sphingomyelins and their corresponding dihydro species, Biophys. J. 80 (2001) 2327–2337.
[39] T. Bartels, R.S. Lankalapalli, R. Bittman, K. Beyer, M.F. Brown, Raftlike mixtures of sphingomyelin and cholesterol investigated by solid-state 2H NMR spectroscopy, J. Am. Chem. Soc. 130 (2008) 14521–14532.
[40] H.A. Scheidt, P. Muller, A. Herrmann, D. Huster, The potential of fluorescent and spin-labeled steroid analogs to mimic natural cholesterol, J. Biol. Chem. 278 (2003) 45563–45569.
[41] S.N. Ahmed, D.A. Brown, E. London, On the origin of sphingolipid/cholesterol-rich detergent-insoluble cell membranes: physiological concentrations of cholesterol and sphingolipid induce formation of a detergent-insoluble, liquid-ordered lipid phase in model membranes, Biochemistry 36 (1997) 10944–10953.
[42] X. Xu, R. Bittman, G. Duportail, D. Heissler, C. Vilcheze, E. London, Effect of the structure of natural sterols and sphingolipids on the formation of ordered sphingolipid/sterol domains (rafts). Comparison of cholesterol to plant, fungal, and disease-associated sterols and comparison of sphingomyelin, cerebrosides, and ceramide, J. Biol. Chem. 276 (2001) 33540–33546.
[43] K.K. Halling, B. Ramstedt, J.H. Nystrom, J.P. Slotte, T.K. Nyholm, Cholesterol interactions with fluid-phase phospholipids: effect on the lateral organization of the bilayer, Biophys. J. 95 (2008) 3861–3871.
[44] T.K. Nyholm, M. Nylund, J.P. Slotte, A calorimetric study of binary mixtures of dihydrosphingomyelin and sterols, sphingomyelin, or phosphatidylcholine, Biophys. J. 84 (2003) 3138–3146.
[45] B. Ramstedt, J.P. Slotte, Interaction of cholesterol with sphingomyelins and acyl-chain-matched phosphatidylcholines: a comparative study of the effect of the chain length, Biophys. J. 76 (1999) 908–915.
[46] D.A. Redfern, A. Gericke, Domain formation in phosphatidylinositol monophosphate/phosphatidylcholine mixed vesicles, Biophys. J. 86 (2004) 2980–2992.
[47] J.P. Bradshaw, R.J. Bushby, C.C. Giles, M.R. Saunders, Orientation of the headgroup of phosphatidylinositol in a model biomembrane as determined by neutron diffraction, Biochemistry 38 (1999) 8393–8401.
[48] P.L. Yeagle, W.C. Hutton, C. Huang, R.B. Martin, Phospholipid head-group conformations; intermolecular interactions and cholesterol effects, Biochemistry 16 (1977) 4344–4349.
[49] G. Cevc, Isothermal lipid phase transitions, Chem. Phys. Lipids 57 (1991) 293–307.
[50] H. Binder, O. Zschornig, The effect of metal cations on the phase behavior and hydration characteristics of phospholipid membranes, Chem. Phys. Lipids 115 (2002) 39–61.
[51] H. Trauble, H. Eibl, Electrostatic effects on lipid phase transitions: membrane structure and ionic environment, Proc. Natl. Acad. Sci. U. S. A 71 (1974) 214–219.
[52] D. Papahadjopoulos, A. Portis, W. Pangborn, Calcium-induced lipid phase transitions and membrane fusion, Ann. N. Y. Acad. Sci. 308 (1978) 50–66.
[53] D. Papahadjopoulos, W.J. Vail, W.A. Pangborn, G. Poste, Studies on membrane fusion. II. Induction of fusion in pure phospholipid membranes by calcium ions and other divalent metals, Biochim. Biophys. Acta 448 (1976) 265–283.
[54] D. Papahadjopoulos, W.J. Vail, C. Newton, S. Nir, K. Jacobson, G. Poste, R. Lazo, Studies on membrane fusion. III. The role of calcium-induced phase changes, Biochim. Biophys. Acta 465 (1977) 579–598.
[55] N. Duzgunes, J. Wilschut, R. Fraley, D. Papahadjopoulos, Studies on the mechanism of membrane fusion. Role of head-group composition in calcium- and magnesium-induced fusion of mixed phospholipid vesicles, Biochim. Biophys. Acta 642 (1981) 182–195.
[56] K.W. Cunningham, G.R. Fink, Ca2+ transport in *Saccharomyces cerevisiae*, J. Exp. Biol. 196 (1994) 157–166.
[57] E. Bicknell-Brown, K.G. Brown, D. Borchman, Atomic and Raman spectroscopy of the dipalmitoylphosphatidic acid-calcium complex and phase transitions, Biochim. Biophys. Acta 862 (1986) 134–140.
[58] Y.J. Bjorkqvist, S. Nybond, T.K. Nyholm, J.P. Slotte, B. Ramstedt, N-palmitoylsulfatide participates in lateral domain formation in complex lipid bilayers, Biochim. Biophys. Acta 1778 (2008) 954–962.
[59] S. Roldan-Vargas, A. Martin-Molina, M. Quesada-Perez, R. Barnadas-Rodriguez, J. Estelrich, J. Callejas-Fernandez, Aggregation of liposomes induced by calcium: a structural and kinetic study, Phys. Rev. E Stat. Nonlin. Soft Matter Phys. 75 (2007) 021912.
[60] M. Rujoi, D. Borchman, D.B. DuPre, M.C. Yappert, Interactions of Ca(2+) with sphingomyelin and dihydrosphingomyelin, Biophys. J. 82 (2002) 3096–3104.
[61] X. Mulet, R.H. Templer, R. Woscholski, O. Ces, Evidence that phosphatidylinositol promotes curved membrane interfaces, Langmuir 24 (2008) 8443–8447.
[62] B. Ramstedt, J.P. Slotte, Sphingolipids and the formation of sterol-enriched ordered membrane domains, Biochim. Biophys. Acta 1758 (2006) 1945–1956.
[63] S.L. Veatch, S.L. Keller, Miscibility phase diagrams of giant vesicles containing sphingomyelin, Phys. Rev. Lett. 94 (2005) 148101.